

Potential Role of PTEN Phosphatase in Ethanol-Impaired Survival Signaling in the Liver

Jong Eun Yeon, Sophia Califano, Julia Xu, Jack R. Wands, and Suzanne M. De La Monte

Chronic ethanol consumption can cause sustained hepatocellular injury and inhibit the subsequent regenerative response. These effects of ethanol may be mediated by impaired hepatocyte survival mechanisms. The present study examines the effects of ethanol on survival signaling in the intact liver. Adult Long Evans rats were maintained on ethanol-containing or isocaloric control liquid diets for 8 weeks, after which the livers were harvested to measure mRNA levels, protein expression, and kinase or phosphatase activity related to survival or proapoptosis mechanisms. Chronic ethanol exposure resulted in increased hepatocellular labeling for activated caspase 3 and nuclear DNA damage as demonstrated using the TUNEL assay. These effects of ethanol were associated with reduced levels of tyrosyl phosphorylated (PY) IRS-1 and PI3 kinase, Akt kinase, and Erk MAPK activities and increased levels of phosphatase tensin homologue deleted on chromosome 10 (PTEN) mRNA, protein, and phosphatase activity in liver tissue. *In vitro* experiments demonstrated that ethanol increases PTEN expression and function in hepatocytes. However, analysis of signaling cascade pertinent to PTEN function revealed increased levels of nuclear p53 and Fas receptor mRNA but without corresponding increases in GSK-3 activity or activated BAD. Although fork-head transcription factor levels were increased in ethanol-exposed livers, virtually all of the fork-head protein detected by Western blot analysis was localized within the cytosolic fraction. In conclusion, chronic ethanol exposure impairs survival mechanisms in the liver because of inhibition of signaling through PI3 kinase and Akt and increased levels of PTEN. However, uncoupling of the signaling cascade downstream of PTEN that mediates apoptosis may account for the relatively modest degrees of ongoing cell loss observed in livers of chronic ethanol-fed rats. (HEPATOLOGY 2003;38:703-714.)

Clinical studies have demonstrated that chronic ethanol consumption can cause chronic liver disease. However, the functional consequences of chronic ethanol abuse can remain subtle over long peri-

ods, indicating an overall high degree of adaptive tolerance to the hepatotoxic effects of ethanol. A number of studies have documented that chronic ethanol exposure impairs liver regeneration following experimental partial hepatectomy. These adverse effects of ethanol have been linked to inhibition of growth factor (mainly insulin and insulin-like growth factor type 1; IGF-1) signaling that mediates DNA synthesis.¹⁻⁴

Insulin and IGF-1 mediate their effects by activating complex intracellular signaling pathways that are initiated by ligand binding to cell surface receptors and attendant activation of intrinsic receptor tyrosine kinases.⁵⁻⁷ Insulin/IGF-1 receptor tyrosine kinases phosphorylate a number of exogenous cytosolic molecules, including one of the major substrates, the insulin receptor substrate type 1 (IRS-1).⁷⁻⁹ Tyrosyl phosphorylated (PY) IRS-1 transmits intracellular signals that mediate growth, survival, and energy metabolism by interacting with downstream molecules that contain *src* homology domains.¹⁰ For example, PY-IRS-1 interacts with the growth-factor receptor-bound protein 2 (Grb2),¹¹ Syp protein tyrosine phosphatase,¹² and the p85 subunit of phosphatidylinositol-3

Abbreviations: IGF-1, insulin-like growth factor type 1; IRS-1, insulin receptor substrate-1; PY, tyrosyl phosphorylated; Grb2, growth factor receptor bound protein 2; PI3K, phosphatidylinositol-3 kinase; MAPK, mitogen-activated protein kinase; HCC, hepatocellular carcinoma; PTEN, phosphatase tensin homologue deleted on chromosome 10; TUNEL, terminal transferase dUTP end-labeling; BCIP/NBT, 5-bromo-4-chloro-3-indolyl phosphate/nitroblue tetrazolium; DU, densitometry units; GSK-3, glycogen synthase kinase-3; RT-PCR, reverse transcription polymerase chain reaction; PCNA, proliferating cell nuclear antigen.

From the Liver Research Center, Departments of Medicine and Pathology, Brown Medical School, Providence, RI.

Received October 10, 2002; accepted June 2, 2003.

Supported by COBRE Grant P20RR15578 from the NIH; AA02666, AA02169, AA11431, and AA12908 from the NIAAA; and the Korean Association Study of Liver Disease Glaxo Wellcome Hepatologist Hepatitis Fellowship Fund (to J.E.Y.)

Address reprint requests to: Suzanne M. de la Monte, M.D., M.P.H. Pierre Galletti Research Building, Rhode Island Hospital, 55 Claverick Street, Room 419, Providence, RI 02903. E-mail: Suzanne_DeLaMonte_MD@Brown.edu; fax: 401-444-2939.

Copyright © 2003 by the American Association for the Study of Liver Diseases.

0270-9139/03/3803-0021\$30.00/0

doi:10.1053/jhep.2003.50368

kinase (PI3K).^{10,13} The binding of PY-IRS-1 to Grb2 results in sequential activation of p21^{ras}, mitogen-activated protein kinase (MAPK) kinase, and Erk MAPK.¹⁴⁻¹⁶ Erk MAPK activation directly contributes to insulin/IGF-1-stimulated mitogenesis and gene expression. The binding of PY-IRS-1 to p85 stimulates glucose uptake and inhibits apoptosis by signaling through Akt/protein kinase B.^{17,18}

Previous studies with hepatocellular carcinoma (HCC)¹⁹ or other cell lines and regenerating liver² demonstrated ethanol inhibition of growth factor receptor tyrosine kinases, Erk MAPK, and second messenger cascades such as calcium phospholipid-dependent protein kinase. These abnormalities were associated with reduced DNA synthesis and cell proliferation and impaired liver regeneration following partial hepatectomy.^{1,2} Therefore, the inhibitory effects of ethanol on hepatocellular growth mechanisms are well established. However, regenerating liver differs from normal liver because of its vastly increased proliferative capacity. To understand better the adverse effects of ethanol, we explored ethanol-mediated abnormalities in intracellular signaling that occur in normal liver and in the absence of exogenous growth stimuli. Previous investigations from our laboratory demonstrated that ethanol inhibition of insulin/IGF-1 signaling through IRS-1 impairs liver regeneration because of decreased DNA synthesis and Erk MAPK activation.¹ Further studies showed that with IRS-1 over expression in either transgenic mice or HCC cell lines, ethanol prominently inhibits growth pathways.^{1,19} The present study demonstrates that chronic ethanol exposure impairs survival mechanisms in the previously normal liver by constitutively inhibiting PI3 kinase activity, an effect that is mediated by increased levels of phosphatase tensin homologue deleted on chromosome 10 (PTEN) phosphatase expression and function.

Materials and Methods

Chronic Ethanol Feeding Model. Adult Long-Evans female rats were fed ethanol-containing (n = 9) or isocaloric control (n = 8) liquid diets (BioServ, Frenchtown, NJ) for 8 weeks. Ethanol comprised 11.8%, 23.6%, and 35.4% of the calorie content of the feedings during the first, second, and third weeks of adaptation, respectively, after which the ethanol-fed rats were maintained on the 35.4% caloric (10% vol/vol) ethanol-containing diet. The preparation of the diets was such that the carbohydrate content was equal in the control and ethanol-containing formulas. This protocol resulted in serum ethanol levels of ~50 mmol/L, which is generally lower than the serum ethanol concentrations found in chronic alcoholics.²⁰ Rats were monitored daily to ensure adequate

nutritional intake and maintenance of body weight. At the end of the feeding period, the rats were killed by i.p. injection of 120 mg/kg sodium pentothal, and liver tissue was snap-frozen in a dry ice/methanol bath or fixed in Histochoice (Amresco, Solon, OH) for histologic studies. This protocol was approved by the subcommittee on Animal Studies at the Rhode Island Hospital and conforms to guidelines established by the National Institutes of Health.

In Situ Assays for Apoptosis. The terminal transferase dUTP end-labeling (TUNEL) assay was used to detect nicked or fragmented DNA in cryostat sections of liver. TUNEL assays were performed using [FITC]dUTP (Gibco-BRL, Grand Island, NY) and terminal deoxynucleotidyl transferase. The FITC-labeled DNA was detected with biotinylated secondary antibody, alkaline phosphatase conjugated Streptavidin, and 5-bromo-4-chloro-3-indolyl phosphate/nitroblue tetrazolium (BCIP/NBT) substrate. To detect nuclear pyknosis and fragmentation characteristic of apoptosis, adjacent sections were stained with Hoechst H33258 (1 μ g/mL in PBS) or propidium iodide (0.5 μ g/mL) for 2 minutes at room temperature. The slides were rinsed thoroughly in PBS, cover-slipped with Vectashield-mounting medium (Vector Laboratories, Burlingame, CA), and examined by fluorescence microscopy. Adjacent sections were immunostained with polyclonal antibodies to activated (cleaved) caspase-3 because caspase-3 is an important effector of apoptosis. The antibodies were generated with a synthetic peptide corresponding to amino-terminal residues adjacent to Asp 175 (Cell Signaling, Beverly, MA). Sections were processed for immunostaining according to the manufacturer's protocol, and immunoreactivity was detected with biotinylated secondary antibody, alkaline phosphatase-conjugated Streptavidin, and the BCIP/NBT substrate.

Protein Studies. Protein expression was examined by Western blot analysis or immunoprecipitation followed by immunoblotting. For direct Western blot analysis, liver tissue was homogenized in 5 volumes of radio-immunoprecipitation assay buffer (50 mmol/L Tris-HCl, pH 7.5, 1% NP-40, 0.25% Na-deoxycholate, 150 mmol/L NaCl, 1 mmol/L EDTA, 2 mmol/L EGTA) containing protease and phosphatase inhibitors (1 mmol/L PMSF, 0.1 mmol/L TPCK, 1 μ g/mL aprotinin, 1 μ g/mL pepstatin A, 0.5 μ g/mL leupeptin, 1 mmol/L NaF, 1 mmol/L Na₄P₂O₇, 2 mmol/L Na₃VO₄). Protein concentrations were determined using the bis-chloracetate assay (Pierce, Rockford, IL). For immunoblotting, samples containing 100 μ g of protein were fractionated by sodium dodecyl sulfate-polyacrylamide gel electrophoresis and transferred to PVDF membranes. Nonspecific binding sites were blocked with SuperBlock-TBS (Pierce), and

the membranes were incubated with primary antibody (0.5-1 $\mu\text{g}/\text{mL}$) overnight at 4°C with gentle agitation. Immunoreactivity was detected with horseradish peroxidase-conjugated secondary antibody and enhanced chemiluminescence reagents and then quantified using the Kodak Digital Science Imaging Station (NEN Life Sciences, Boston, MA). Levels of immunoreactivity are reported in arbitrary densitometry units (DU).

For immunoprecipitation studies, liver tissue was homogenized in Triton lysis buffer (50 mmol/L Tris-HCl, pH 7.5, 10 mmol/L EDTA, 1% Triton X-100) containing protease and phosphatase inhibitors as indicated above. Aliquots of 500 μg protein diluted to 1 mg/mL in Triton lysis buffer were precleared with Protein A sepharose (Amersham, Pharmacia) then incubated overnight at 4°C with 1 $\mu\text{g}/\text{mL}$ of primary antibody using constant rotation of the samples. Protein A sepharose was then added, and the samples were further incubated for 2 hours at 4°C with constant rotation. The immune complexes were washed 3 times in Triton lysis buffer using a standard protocol.²¹ After the third wash, the immunoprecipitants were either resuspended in sodium dodecyl sulfate polyacrylamide gel electrophoresis sample buffer with loading dye²¹ for Western blot analysis, or they were processed further to assay kinase or phosphatase activity.

Assays of Kinase Activity. PI3K activity was measured in IRS-1 and p85 immunoprecipitates containing 0.1 mol/L Tris-HCl, pH 7.4, 5 mmol/L LiCl, and 0.1 mmol/L sodium orthovanadate. After the third wash in Triton lysis buffer, the immune complexes were washed 3 times in buffer containing 0.1 mol/L Tris-HCl, pH 7.4, 5 mmol/L LiCl, and 0.1 mmol/L sodium orthovanadate and then twice with Tris-sodium chloride-EDTA buffer (TNE; 10 mmol/L Tris-HCl, pH 7.4, 150 mmol/L NaCl, 5 mmol/L EDTA, 0.1 mmol/L sodium orthovanadate). The immunoprecipitates were suspended in 25 μL TNE, and reactions were initiated by the addition of 10 μL sonicated phosphatidylinositol (20 μg per reaction), 10 μL of 100 mmol/L MgCl_2 , and 5 μL ATP reaction mixture (0.88 mmol/L ATP, 30 μCi [$\gamma^{32}\text{-P}$]ATP [3,000 Ci/mmol], 20 mmol/L MgCl_2). Reactions were incubated for 10 minutes at 37°C and stopped by adding 20 μL of 6 N HCl. Lipids were extracted with 1:1 CHCl_3 :MeOH, spotted on oxalate-treated silicon TLC plates (Merck, White House Station, NJ) and fractionated by chromatography. PI3K activity was detected by film autoradiography and quantified using the Kodak Digital Science Imaging Station.

Erk MAPK, Akt kinase, and glycogen synthase kinase 3 (GSK-3) kinase activities were measured in corresponding immunoprecipitates obtained from 500 μg protein samples. The immunoprecipitates captured onto Protein

Table 1. Forward and Reverse Primer Sequences for Real-Time RT-PCR

Primer	Sequence (5'-3')	PCR Product (bp)
PTEN for	GGA AAG GAC GGA CTG GTG TA	163
PTEN rev	TGC CAC TGG TCT GTA ATC CA	
TPIP for	TAT TCT GAT AG AAT TTT TCA TCT GC	95
TPIP rev	CCT CGG CAG TTA AAA ATA TTT CG	
Fas R for	GCA ATG CTT CTC TCT GTG ACC ACT G	374
Fas R rev	GCT GTT GTG CTC GAT CTC ATC G	
Fas L for	ATA GAG CTG TGG CTA CCG GTG	286
Fas L rev	CTC GAG AGA TCA AAG CAG TTC C	
18s for	GGA CCA GAG CGA AAG CAT TTG CC	495
18s rev	TCA ATC TCG GGT GGC TGA ACG C	

Abbreviations: for, forward; rev, reverse.

A sepharose were washed 3 times with Triton lysis buffer and twice with assay dilution buffer (ADB; 20 mmol/L MOPS, pH 7.2, 25 mmol/L β -glycerol phosphate, 5 mmol/L EGTA, 1 mmol/L sodium orthovanadate, 1 mmol/L dithiothreitol) and then resuspended in 10 μL of ADB. Reactions were initiated by adding 10 μL of kinase peptide substrate followed by 10 μL ATP/mg cocktail ([$\gamma^{32}\text{-P}$]ATP, 75 mmol/L MgCl_2 , 500 $\mu\text{mol}/\text{L}$ cold ATP). Myelin basic protein peptide (250 $\mu\text{mol}/\text{L}$) was used to measure Erk MAPK activity; Crosstide (100 $\mu\text{mol}/\text{L}$) was used to measure Akt kinase, and CREB (200 $\mu\text{mol}/\text{L}$) was used to measure GSK-3 activity. Reactions were incubated for 10 or 15 minutes at 30°C with agitation and stopped by adding 5 μL of 0.5 mol/L EDTA. The reaction products were blotted onto p81 phosphocellulose, and unincorporated [$\gamma^{32}\text{-P}$] ATP was removed by washing the filters with 0.85% phosphoric acid. [$\gamma^{32}\text{-P}$] Incorporation was measured in a TopCount machine (Packard Instrument Co. Meriden, CT).

In Vivo PTEN Studies. Using rat liver tissue, PTEN expression was measured by Western blot analysis and real-time quantitative reverse-transcription polymerase chain reaction (RT-PCR). For the RT-PCR studies, RNA was isolated from liver tissue homogenates using TRIZOL reagent (Invitrogen, Carlsbad, CA) according to the manufacturer's protocol. Samples containing 1 μg RNA were reverse transcribed using the AMV First Strand cDNA synthesis kit (Roche, Basel, Switzerland) and random oligodeoxynucleotide primers. cDNA fragments isolated from HepG2 cells by RT-PCR were cloned into the PCR II vector (Invitrogen, Carlsbad, CA) and used to generate standard curves for determining transcript abundance. PCR amplifications were performed using 25 μL reactions containing RT product generated from 10 ng of template, 300 nmol/L each of forward and reverse primers (Table 1) and SYBR Green I PCR reagents (Applied Biosystems, Foster, CA). The am-

plified signals were detected continuously with the Bio-Rad iCycler and iCycler iQ Multi-Color Real Time PCR Detection System (Hercules, CA). The following real-time PCR amplification protocol was used: (1) an initial denaturation of 95°C for 10 minutes; (2) a 3-segment amplification and quantification program consisting of 40 cycles of 95°C × 60 seconds, 60°C × 45 seconds, and 72°C for 30 seconds; and (3) a final extension at 72°C for 10 minutes.

In Vitro PTEN Studies. To directly evaluate the effects of ethanol on PTEN expression and functional activity in hepatocytes, primary cultures were generated with hepatocytes isolated from chronic ethanol-fed and control animals using the collagenase perfusion method.²² The cultures were maintained in humidified chambers with 50 mmol/L or no ethanol included in the reservoir tray. The objective was to maintain the chronic ethanol exposure state and simulate *in vivo* conditions. The studies did not include analysis of ethanol withdrawal or acute ethanol exposure because the objective was to determine whether the *in vivo* effects of chronic ethanol exposure on PTEN expression and phosphatase activity were due to responses occurring in hepatocytes. After 24 hours in culture, the cells were harvested for assays of PTEN expression, phosphorylation, and phosphatase activity. Protein concentration was measured using the bis-chloracetate assay. PTEN protein expression, phosphorylation, and phosphatase activity were measured in 30 µg samples of total protein. PTEN phosphorylation was detected by Western blot analysis of antiphosphoserine/phosphothreonine immunoprecipitates. PTEN phosphatase activity was measured in PTEN immunoprecipitates using the Biomol Green Reagent according to the manufacturer's protocol (Biomol, PA). The specificity of the Biomol Green assay is dependent on the use of immunoprecipitates rather than tissue or cellular homogenates.

Source of Reagents. Antibodies to Akt, GSK-3, BAD, PTEN, Phospho-Akt, phospho-GSK-3β (Ser⁹), and phospho-BAD (Ser¹¹²) were purchased from Cell Signaling Technology (Beverly, MA). Antibodies to IRS-1, p85 subunit of PI3K, and phosphotyrosine (PY20) were purchased from Transduction Laboratories (Lexington, KY). MAP kinase substrate peptide and Crosstide were purchased from Upstate Biotechnology (Lake Placid, NY). CREB was obtained from New England Biolabs (Beverly, MA). Phosphoserine and phosphothreonine antibodies and phosphatidylinositol were purchased from Sigma-Aldrich, Inc. (St. Louis, MO).

Statistical Analysis. Data depicted in the graphs represent mean ± SEM. Intergroup comparisons were made with Student's *t* tests.

Results

Increased Apoptosis Proneness in Livers From Ethanol-Fed Rats. Histologic sections of liver demonstrated microvesicular lipid accumulation in hepatocytes of ethanol-fed rats as previously described.¹ Necrotic foci were rare and inconspicuous. Therefore, our studies were focused on ethanol-induced apoptosis and proapoptosis/antisurvival mechanisms. Immunohistochemical staining studies demonstrated increased hepatocellular expression of activated (cleaved) caspase-3, and TUNEL assay staining revealed increased nuclear labeling in livers from ethanol-exposed relative to control rats (Fig. 1). In the ethanol-exposed livers, activated caspase-3 was mainly localized in the nucleus, although peripheral membranous labeling was also detected (Fig. 1B). Previous studies showed that nuclear translocation is required for caspase induction of apoptosis.²³ Together with the finding of increased nuclear labeling by the TUNEL assay, which reflects genomic DNA damage, these results demonstrate that chronic ethanol feeding promotes hepatocellular injury with apoptotic cell loss and remodeling in the livers of Long Evans rats.

Ethanol Inhibits Signaling Through IRS-1. Previous *in vitro* studies showed that growth factor signaling through IRS-1 mediates growth and survival and that ethanol inhibits insulin and IGF-1 stimulated signaling *in vitro*.¹⁻⁴ To determine whether chronic ethanol feeding impairs IRS-1 mediated signaling *in vivo*, the levels of PY-IRS-1 and total IRS-1 protein were measured in liver tissue by Western blot analysis of IRS-1-immunoprecipitates and direct immunoblotting. The studies revealed 64.8% lower mean levels of PY-IRS-1 in livers from ethanol-exposed relative to control rats ($P = .008$) but similar levels of total IRS-1 protein (~185 kd) in both groups (Fig. 2).

Chronic Ethanol Feeding Inhibits Progrowth Signaling in the Liver. Growth factor signaling through IRS-1 mediates cell growth by activating the Ras-Raf-Erk MAPK pathway. Because previous studies correlated ethanol-impaired liver regeneration with inhibition of IRS-1-transmitted signaling through Erk MAPK,^{10,12,13,15} it was of interest to determine whether the reduced levels of PY-IRS-1 in ethanol-exposed livers were associated with inhibition of Erk MAPK. Hepatic Erk MAPK activity was significantly reduced (~24% lower) in the ethanol-fed relative to control samples (Fig. 3A; $P = .001$), whereas Erk protein expression was similar in control and ethanol-exposed livers as demonstrated by Western blot analysis with digital image quantification (Fig. 3B). However, ethanol inhibition of Erk MAPK was not associated with

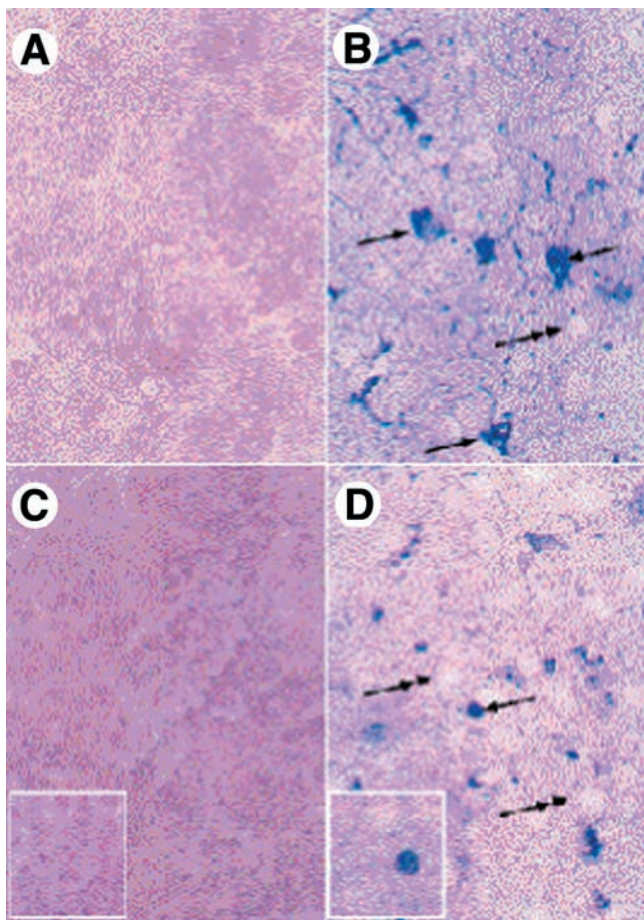


Fig. 1. Ethanol-induced hepatocellular apoptosis proneness. Histologic sections were immunostained to detect activated (cleaved) caspase-3 (A and B) or used in TUNEL assays to detect nicked or fragmented nuclear DNA (C and D). Immunoreactivity and end-labeled DNA were detected with biotinylated secondary antibody, alkaline phosphatase-conjugated Streptavidin, and BCIP/NBT substrate (blue precipitate). Livers from control rats (A and C) had no detectable activated caspase-3 or TUNEL+ labeling in hepatocytes. In contrast, livers from ethanol-fed rats had scattered hepatocytes with immunoreactivity for activated caspase-3 both at cell membrane borders and within the nuclei (B) and TUNEL+ labeling of nuclei (D) (arrows). Insets in panels C and D show higher magnification images of the TUNEL assay results. Double-headed arrows in panels B and D point toward lipid-laden vacuoles in hepatocytes of ethanol-fed rats.

reduced levels of proliferating cell nuclear antigen (PCNA) expression (Fig. 3C).

Chronic Ethanol Exposure Inhibits PI3K. Growth factor-stimulated survival is mediated by activation of PI3K, which can involve either IRS-1-dependent or IRS-1-independent pathways,^{24,25} and previous *in vitro* studies demonstrated that ethanol impairment of viability associated with inhibition of growth factor stimulated PI3K activity.^{1,12,13} To determine the mechanism by which chronic ethanol exposure inhibits survival *in vivo*, PI3K activity was measured in both IRS-1 and p85 immunoprecipitates. In addition, because IRS-1-associated

PI3K is reflected by the degree of interaction between p85 and IRS-1, p85-associated IRS-1 levels were examined by Western blot analysis of IRS-1 immunoprecipitates. Those studies demonstrated similar levels of IRS-1-associated p85 and IRS-1-associated PI3K activity in control and ethanol-exposed livers (Fig. 4A, B, and D) but strikingly reduced levels (85.4% lower) of total PI3K activity in ethanol-fed relative to control livers ($P = .001$; Fig. 4C and E), consistent with previous results obtained using a CD rat model of chronic ethanol feeding.²

Ethanol-Induced PTEN Expression In Vivo. PTEN is a negative regulator of PI3K-mediated cell growth and survival signaling. PTEN functions by dephosphorylating the third position of phosphatidylinositide. In previous studies, which employed an IRS-1-over expressing transgenic mouse model¹ or HCC cell lines,²⁴ ethanol inhibition of PI3K was linked to impaired signaling through IRS-1. Because results from the present investigations indicated that, in the normal liver, ethanol-induced hepatocellular injury associated with inhibition of PI3K mainly involves IRS-1-independent pathways, we were led to explore the role of PTEN as a potential inhibitor of PI3K-mediated survival.

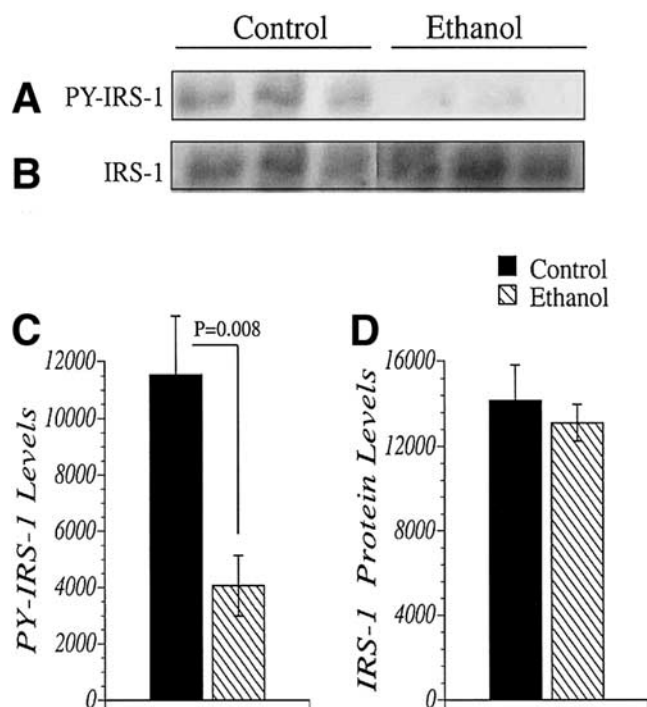


Fig. 2. Reduced levels of tyrosyl phosphorylated (PY) insulin receptor substrate type 1 (IRS-1) in the livers of ethanol exposed relative to control rats. (A) Representative anti-PY Western blot results of IRS-1 immunoprecipitates of liver tissue. (B) Representative direct Western blotting results showing IRS-1 protein expression in liver tissue. Each lane corresponds to an individual rat, and 10 rats were analyzed in each group. (C and D) Western blot signals were quantified using the Kodak Digital Image Station, and results (mean \pm SEM) are depicted graphically.

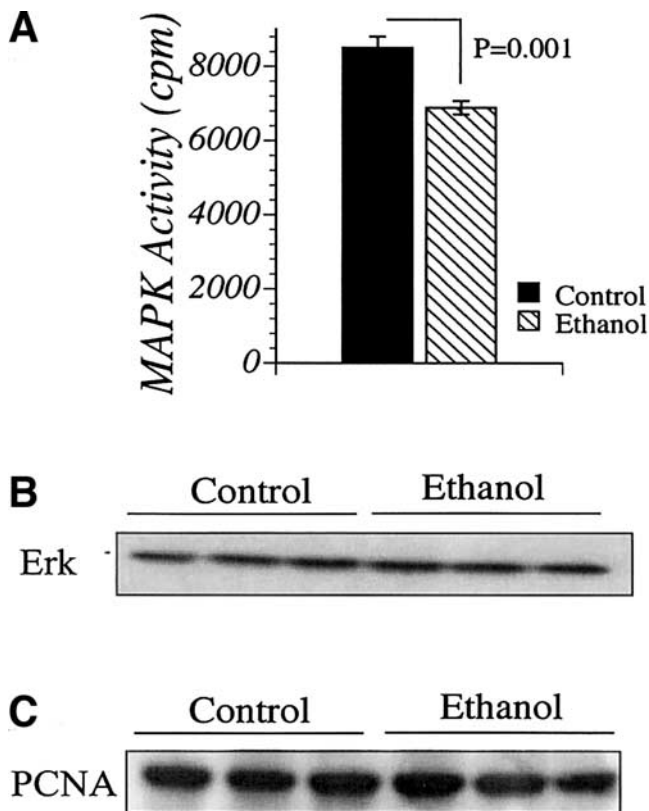


Fig. 3. Ethanol inhibition of Erk MAPK activity. Erk MAPK activity was measured in total Erk immunoprecipitates from liver tissue homogenates using a myelin basic protein peptide-based assay. [γ - 32 P]ATP incorporation was measured in a TopCount machine. Graphed data represent the mean \pm SEM of results from each group. (B and C) Western blot analysis demonstrating similar levels of Erk and PCNA protein expression in livers from control and ethanol-fed rats.

Western blot analysis detected the expected \sim 54 kD PTEN protein in all samples (Fig. 5A). In addition, a second, slower migrating band was detected, and, recently, a PTEN isoform, TPIP, was identified.²⁶ Digital image quantification of the Western blot signals demonstrated significantly higher mean levels of PTEN and TPIP in ethanol-fed relative to control livers (Fig. 5B and C). Because previous reports demonstrated that phosphorylation of PTEN inhibited its phosphatase activity,^{27,28} further studies examined the levels of phospho-PTEN by antiphosphoserine/phosphothreonine Western blot analysis of PTEN immunoprecipitates (Fig. 5A). Those studies demonstrated reduced levels of phospho-PTEN in livers from ethanol-fed ($52,238 \pm 1,200$ DU) relative to control ($80,999 \pm 4,502$ DU) rats ($P = .003$). In addition, the samples from ethanol-fed rats had significantly increased levels of phosphatase activity in PTEN immunoprecipitates (Fig. 5D).

Real-time quantitative RT-PCR studies were used to determine whether PTEN and TPIP mRNA levels were increased in ethanol-exposed livers. PTEN, TPIP, and

18s RNA transcripts were simultaneously evaluated in parallel reactions using aliquots of the same cDNA templates. Serial dilutions of known quantities of recombinant plasmid DNA containing PTEN, TPIP, or 18s cDNA target fragments were used as standards in all PCR reactions, and the regression lines generated with the C_t values of the standards were used to calculate mRNA abundance. The results were normalized with respect to 18s RNA because the expression levels of various house-keeping genes were found to be altered in ethanol-exposed livers. Between-group comparisons (Student's t test) were made using the calculated PTEN/18s and TPIP/18s ratios. The studies revealed significantly increased levels of both PTEN and TPIP mRNA transcripts in livers from ethanol-fed relative to control rats (Fig. 5E and F).

Ethanol-Induced PTEN Expression In Vitro. Additional *in vitro* experiments were performed to determine whether ethanol exposure inhibited PI3K activity and in-

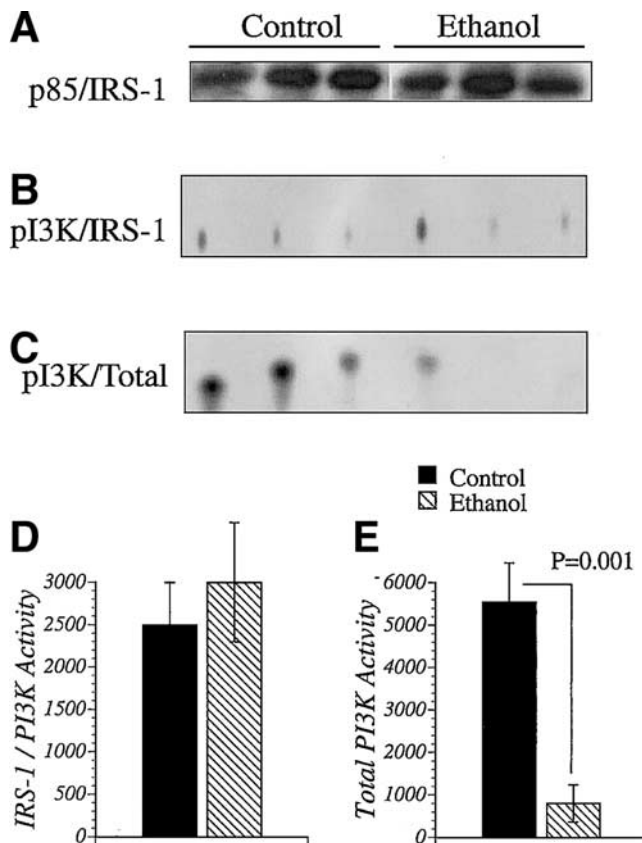


Fig. 4. Ethanol inhibition of PI3K activity. (A) Western blot analysis of p85-associated IRS-1 protein. (B) PI3K activity measured in IRS-1 immunoprecipitates from liver homogenates. (C) Total PI3K activity measured in p85 immunoprecipitates. Kinase activity was measured with a standard phospholipid-based phosphorylation assay. (D and E) Graphs depict the mean levels (\pm SEM) of [γ - 32 P]ATP incorporation measured by digital image quantification of the autoradiographic signals using the Kodak Digital Science Image Station.

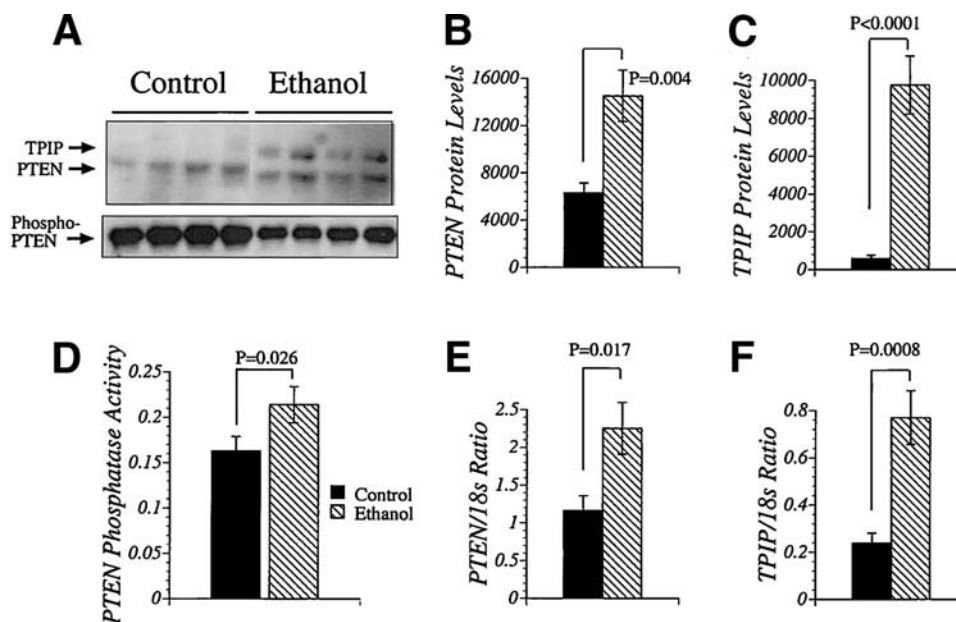


Fig. 5. Increased PTEN phosphatase expression in liver tissue from ethanol exposed rats. (A) Western blot autoradiograph demonstrating expression of the PTEN and TPIP proteins in liver homogenates. (B and C) Graphs depict the mean levels (\pm SEM) of PTEN or TPIP measured by digital image analysis of the Western blot signals. (D) Levels of PTEN phosphatase activity measured in immunoprecipitates using the Biomol Green assay. (E and F) Real-time quantitative RT-PCR was used to examine mRNA levels of PTEN, TPIP, and 18s. The actual levels of expression were determined from standard curves generated with recombinant plasmid DNA. PTEN and TPIP mRNA levels were normalized to 18s to control for slight differences in template loading or cellular RNA abundance. The graphs depict the mean \pm SEM of the calculated PTEN/18s and TPIP/18s copy number ratios for each group.

creased PTEN expression and phosphatase activity in hepatocytes. Corresponding with the *in vivo* observations, PI3K activity was significantly reduced in hepatocyte cultures generated from ethanol-fed (51.4 ± 0.45 DU) relative to control (79.3 ± 0.16 DU) rats ($P = .001$). Western blot analysis demonstrated higher levels of PTEN protein expression in hepatocytes from ethanol-exposed relative to control livers (Fig. 6A and B; $P = .006$). However, the TPIP band detected in liver tissue was not observed in the cultured hepatocytes. Ethanol exposure was also associated with significantly increased levels of PTEN phosphatase activity (Fig. 6C; $P = .026$). Corresponding with the *in vivo* results, antiphosphoserine/phosphothreonine Western blot analysis of PTEN immunoprecipitates demonstrated reduced levels of phospho-PTEN in hepatocytes from ethanol-fed (670.1 ± 19.5 DU) relative to control (590.5 ± 30.4 DU) livers ($P = .014$).

Ethanol Inhibits Signaling Downstream of PI3K. PI3K promotes survival by phosphorylating Akt (protein kinase B) and activating its kinase. Akt kinase phosphorylates GSK-3 and BAD, rendering them inactive. Catalytically active GSK-3 and BAD are proapoptotic. To evaluate survival signaling downstream of PI3K, we examined the levels of Akt, phospho-Akt, Akt kinase, GSK-3 kinase, BAD and phospho-BAD. Total protein

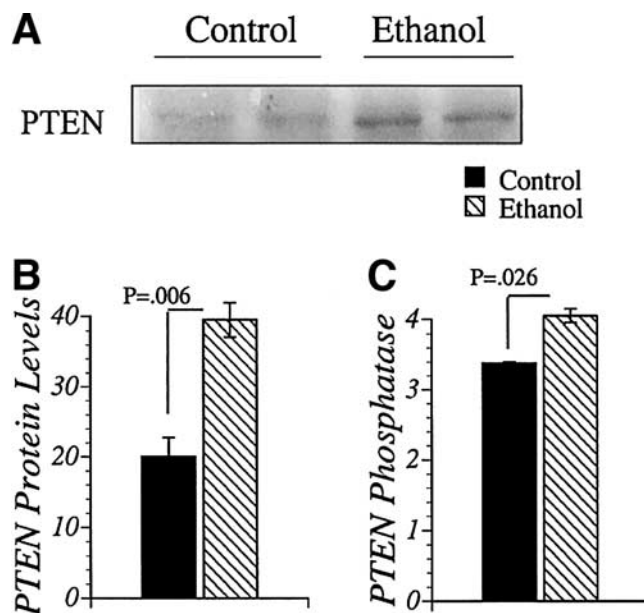


Fig. 6. Ethanol induced PTEN expression in hepatocytes cultured from ethanol-fed and control animals. (A) Example Western blot showing expression of the \sim 54 kD PTEN protein in hepatocytes isolated from individual control or ethanol-exposed rats. (B) The levels of PTEN protein were measured by digital imaging, and the results (mean \pm SEM) are depicted graphically. (C) PTEN phosphatase activity was measured in PTEN immunoprecipitates using the Biomol malachite green-based assay, which detects nanomoles of phosphate released.

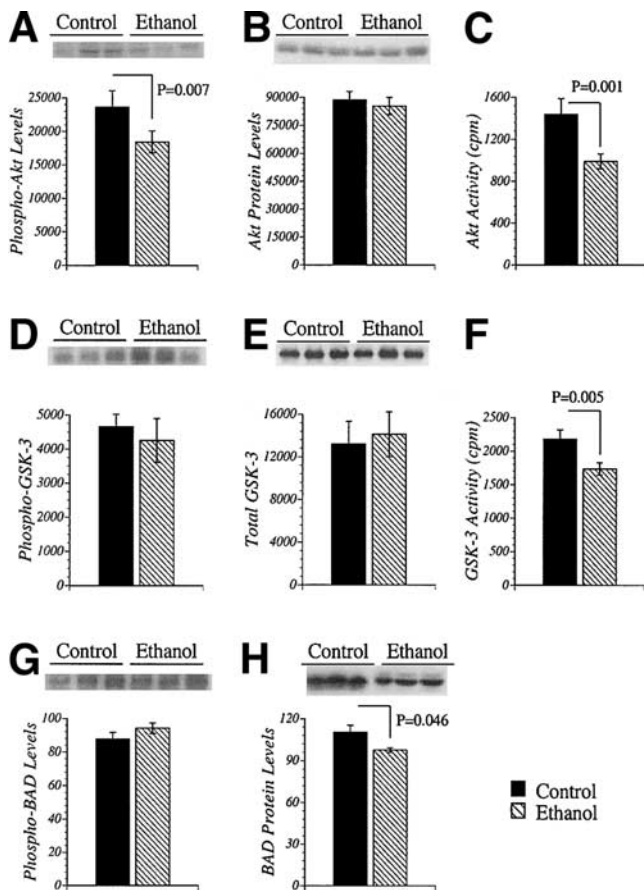


Fig. 7. Ethanol impairs signaling downstream of PI3K in the liver. (A) Phospho-Akt, (B) Akt, (D) phospho-GSK3, (E) total GSK3, (G) phospho-BAD, and (H) total BAD protein levels were measured by Western blot analysis and digital image quantification. Phosphoproteins were detected with phospho-specific antibodies. Representative autoradiographs are shown above each graph. (C) Akt kinase and (F) GSK-3 kinase activities were measured in corresponding immunoprecipitates using cross tide and CREB as peptide substrates for phosphorylation. [γ - 32 P]ATP incorporation was measured in a TopCount machine. Graphs depict the mean \pm SEM of representative results.

and phosphoprotein expression were examined by Western blot analysis, and kinase activity was measured in corresponding immunoprecipitates using specific peptide substrates. The ethanol-fed rats had significantly reduced hepatic levels of phospho-Akt and Akt kinase activity but unaltered levels of Akt protein relative to control samples (Fig. 7A-C). In contrast, the mean levels of phospho-GSK-3 (inactive), total GSK-3, and activated BAD in ethanol-exposed livers were not significantly different from control, and GSK-3 activity was slightly reduced (Fig. 7D-H).

Mechanism of Uncoupled Proapoptosis Signaling.

One would have predicted the ethanol-induced increases in activated caspase 3 and TUNEL+ nuclear labeling in the liver, reductions in PI3K activity, and increased levels of PTEN protein and phosphatase activity to be associ-

ated with inhibition of Akt kinase and increased levels of GSK-3 activity. The results showed inhibition of Akt kinase and, paradoxically, reduced levels of GSK-3 activity. Therefore, further studies were needed to characterize the functional integrity of the signaling pathways related to PTEN expression and function. Corresponding with the increased levels of PTEN mRNA and known transcriptional regulation of PTEN by p53,²⁹ Western blot analysis of nuclear and cytosolic extracts demonstrated significantly increased levels of nuclear p53 in the livers of ethanol-fed rats (Fig. 8A).

Akt promotes survival by phosphorylating fork-head transcription factor leading to its interaction with 14-3-3

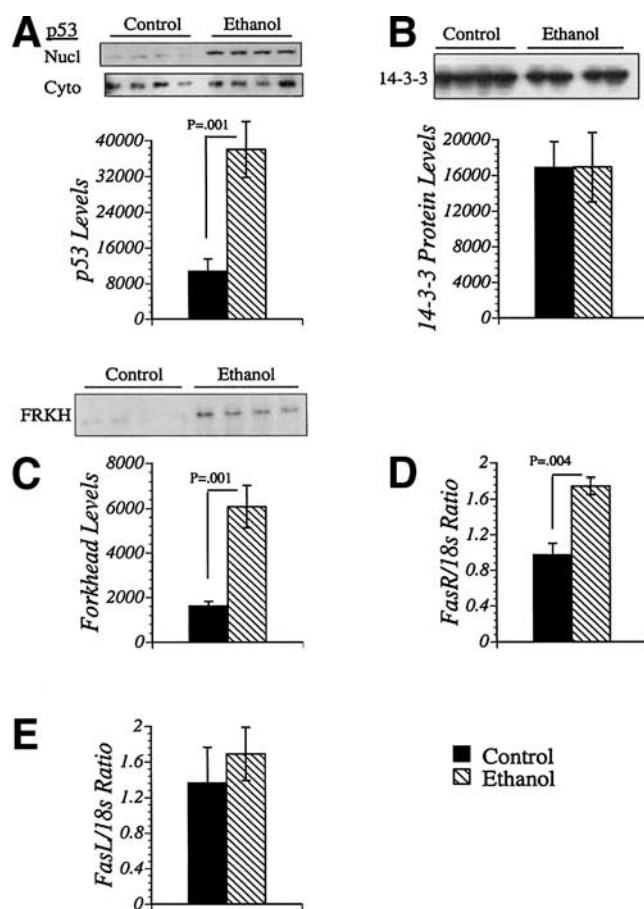


Fig. 8. Effects of chronic ethanol feeding on PTEN-related signaling mechanisms. (A-D) Protein expression was measured by Western blot analysis with digital image quantification of the autoradiographic signals. Example autoradiographs are shown above each of the graphs. (A) p53 Protein detected in the nuclear and cytosolic fractions of liver tissue homogenates. The graph below indicates the levels of p53 measured in the nuclear fractions. (B) 14-3-3 Protein expression in liver tissue homogenates. (C) The Western blot and graph depict fork-head protein levels in the cytosolic fractions of the liver homogenates. In the nuclear fraction, fork-head protein levels were very low and scarcely detectable (data not shown). (D and E) Fas receptor (FasR) and Fas ligand (FasL) mRNA levels were measured using real-time quantitative RT-PCR, and the values were normalized to 18s, which was simultaneously measured in parallel reactions.

and retention in the cytoplasm.³⁰ Therefore, ethanol inhibition of Akt results in increased levels of unphosphorylated fork head, allowing it to translocate to the nucleus and promote transcription of FasL.^{30,31} Western blot analysis revealed similar levels of 14-3-3 in livers from control and ethanol-fed rats (Fig. 8B). Fork-head transcription factor was also more abundantly expressed in the livers from ethanol-fed rats (Fig. 8C), but virtually all of the fork-head protein detected was distributed in the cytosolic rather than nuclear fraction. Nuclear fork-head expression was either very low level or undetectable in both control and ethanol-exposed livers, and, therefore, the 2 groups could not be distinguished on the basis of this parameter (data not shown). Correspondingly, the levels of FasL mRNA were similar in ethanol-exposed and control samples. In contrast, FasR mRNA expression was significantly increased in the ethanol-exposed relative to the control livers, consistent with results from previous studies demonstrating p53 induction of FasR (Fig. 8D and E).³²⁻³⁴

Discussion

One objective of our research was to investigate the *in vivo* effects of ethanol on IRS-1-mediated growth and survival signaling in the normal liver since previous experiments were conducted using isolated cultured hepatocytes, transformed hepatic cell lines, rats subjected to partial hepatectomy, or transgenic mice that over expressed IRS-1 in the liver. A second objective was to determine whether chronic ethanol feeding inhibited survival mechanisms in the liver. To conduct these studies, it was necessary to examine protein phosphorylation, kinase activity, and phosphatase activity in fresh tissue homogenates with rapid processing of samples in buffers supplemented with ample concentrations of protease and phosphatase inhibitors. Using this approach, we detected significantly reduced levels of PY-IRS-1 and normal levels of total IRS-1 protein in livers from ethanol-fed rats. Because these abnormalities occurred without exogenous growth factor stimulation, it is likely that ethanol constitutively inhibits signaling through IRS-1 pathways in the liver.

The finding of reduced Erk MAPK activity in livers of ethanol-fed rats indicates that chronic ethanol exposure constitutively inhibits hepatocellular growth mechanisms, consistent with previous observations in ethanol-exposed IRS-1 transgenic mice¹ and ethanol-treated HCC cell lines.¹⁹ Because the levels of PY-IRS-1 were reduced by chronic ethanol feeding, the associated inhibition of Erk MAPK may have been mediated by reduced interaction between PY-IRS-1 and Grb2, which normally transmits signals downstream through Ras/Raf/MAPK.

The finding that PCNA expression was unaffected by chronic ethanol exposure was not surprising because a potent stimulus for hepatocellular proliferation, such as partial hepatectomy, had not been provided. Nonetheless, the results suggest that the potential for liver regeneration and repair in the intact liver was compromised by the chronic ethanol exposure. Moreover, because other substrates for Erk MAPK, including the transcription factor *elk-1/p62^{TCF}*, *c-jun*, *c-myc*, *NF-IL6*, *TAL1*, RNA polymerase II, *pp90^{rsk}*, cytosolic phospholipase A2, and *raf-1* are expressed in the liver, ethanol inhibition of Erk MAPK could also interfere with basal functions linked to these molecules.

Previous studies using IRS-1 transgenic mice or HCC cell lines revealed that ethanol inhibition of IRS-1 tyrosyl phosphorylation reduced IRS-1-associated PI3K activity. This effect was likely due to ethanol inhibition of tyrosyl phosphorylation at the ⁶¹³YMPM and ⁹⁴²YMKM motifs of IRS-1, resulting in reduced binding of the p85 subunit, which is required for activation of PI3K. In contrast to previous observations, the hepatic levels of IRS-1-associated p85 and IRS-1-associated PI3K activity were not reduced by chronic ethanol feeding, whereas the total PI3K activity was substantially inhibited by ethanol. This discrepancy could be explained by the fact that previous studies employed models in which IRS-1 was over expressed either as a transgene or in association with hepatocellular transformation, whereas, in the normal liver, IRS-1 is expressed at relatively low levels. This suggests that, in the normal liver, IRS-1-independent survival mechanisms may be more important and perhaps more sensitive to the inhibitory effects of ethanol on PI3K signaling than are the less prominent IRS-1-dependent pathways.

PI3K inhibits apoptosis by activating Akt/protein kinase B,^{17,18,35,36} which phosphorylates GSK-3³⁷⁻³⁹ and BAD,⁴⁰ rendering them inactive. Low levels of Akt kinase and high levels of GSK-3 or activated BAD are associated with increased cell death. Activated BAD promotes apoptosis by forming heterodimers with the Bcl-2 and Bcl-XL prosurvival molecules^{41,42} or by disrupting mitochondrial membrane permeability and promoting cytochrome c release and caspase activation. GSK-3 inhibits survival by phosphorylating cytoskeletal proteins that regulate cell process extension, intracellular transport, and maintenance of cell-cell connections.^{37,39,43,44} Our work demonstrates that chronic ethanol exposure results in inhibition of hepatic Akt kinase activity, corresponding with the reduced levels of PI3K.

Consideration of other potential mechanisms by which survival signaling might be inhibited by ethanol led to the examination of PTEN expression in the livers.^{45,46}

PTEN is a lipid phosphatase that dephosphorylates and reverses the activation of PI3K.⁴⁶⁻⁵⁰ Inactivation of PTEN leads to membrane recruitment and increased phosphorylation of Akt, with attendant activation of Akt kinase.^{47,49} In contrast, high levels of PTEN are associated with reduced levels of Akt and increased levels of GSK-3 activity,⁵¹ thereby inhibiting growth and survival mechanisms. Our *in vivo* studies demonstrated significantly increased levels of PTEN mRNA, protein expression, and phosphatase activity and reduced levels of phospho-PTEN in ethanol-exposed livers. Therefore, in addition to higher levels of gene expression, the increased levels of PTEN phosphatase activity may have been partly mediated by ethanol inhibition of PTEN phosphorylation because phosphorylation reduces the enzymatic activity of PTEN.^{27,28} The *in vivo* effects of ethanol on PTEN expression and function were confirmed by *in vitro* experiments.

The studies herein demonstrated dual mechanisms by which chronic ethanol feeding results in inhibition of Akt phosphorylation and kinase activity in the liver: One pathway is linked to impaired growth factor signaling through PI3 kinase, and the other pertains to the regulation of PTEN expression and function. Akt kinase is an important mediator of hepatocellular growth and survival, and, correspondingly, ethanol inhibition of Akt was associated with increased apoptosis in the liver. Akt mediates survival by phosphorylating and inhibiting GSK-3,^{39,51} BAD,⁴⁰ and fork-head transcription factors.^{30,31,52} Therefore, we expected that ethanol activation of PTEN and inhibition of Akt would be associated with increased levels of GSK-3 activity and activated BAD. However, paradoxically, the proapoptosis pathways downstream of Akt were not activated in the ethanol-exposed livers as was evidenced by the absence of ethanol-associated increases in GSK-3 activity and activated BAD expression. Moreover, although fork-head expression was increased, the protein was largely retained in the cytosol rather than translocated to the nucleus where it could up-regulate proapoptosis molecules such as FasL.³⁰ Correspondingly, we did not detect increased levels of FasL mRNA in the ethanol-exposed livers. These findings suggest that the proapoptosis signaling cascades induced by chronic ethanol feeding were partially blocked or uncoupled. With regard to potential mechanisms, a recent study demonstrated that transcriptional up-regulation of FasR leads to inhibition of GSK-3 activity.⁵³ In the present study, we observed increased levels of FasR expression in livers from chronic ethanol-fed rats.

Previous studies demonstrated ethanol-induced oxidative stress associated with increased p53 expression and DNA damage.⁵⁴⁻⁵⁷ Up-regulation of p53 induces FasR

expression and promotes apoptosis.^{32-34,58} Results from the present studies showed that chronic ethanol exposure leads to increased expression of p53, FasR, and PTEN and increased PTEN phosphatase activity and inhibition of survival signaling through PI3 kinase/Akt. Therefore, following chronic ethanol exposure, several proapoptosis/antisurvival mechanisms become activated in the otherwise normal liver. In this context, one would anticipate chronic ethanol feeding to render the liver more susceptible to any second insult that promotes cell loss such as hepatitis B or hepatitis C virus infection. However, we also obtained evidence that, with chronic ethanol feeding, compensatory mechanisms become activated that effectively uncouple or inhibit downstream proapoptosis/antisurvival signaling. In particular, the inhibition of GSK-3, which could be attributed to increased levels of FasR, may have helped to protect the ethanol-exposed livers from more extensive programmed cell death and attendant loss of function. According to this analytical scheme, we predict that, with chronic ethanol feeding, factors or agents that promote FasL expression or GSK-3 activity would reverse or override endogenous compensatory prosurvival mechanisms and result in a greater severity of hepatocellular injury than occurs in the absence of chronic ethanol exposure.

References

- Mohr L, Tanaka S, Wands JR. Ethanol inhibits hepatocyte proliferation in insulin receptor substrate 1 transgenic mice. *Gastroenterology* 1998;115:1558-1565.
- Sasaki Y, Wands JR. Ethanol impairs insulin receptor substrate-1 mediated signal transduction during rat liver regeneration. *Biochem Biophys Res Commun* 1994;199:403-409.
- Seiler AE, Ross BN, Rubin R. Inhibition of insulin-like growth factor-1 receptor and IRS-2 signaling by ethanol in SH-SY5Y neuroblastoma cells. *J Neurochem* 2001;76:573-581.
- Xu YY, Bhavani K, Wands JR, de la Monte SM. Ethanol inhibits insulin receptor substrate-1 tyrosine phosphorylation and insulin-stimulated neuronal thread protein gene expression. *Biochem J* 1995;310:125-132.
- Myers MG, Sun XJ, White MF. The IRS-1 signaling system. *Trends Biochem Sci* 1994;19:289-293.
- O'Hare T, Pilch PF. Intrinsic kinase activity of the insulin receptor. *Int J Biochem* 1990;22:315-324.
- Ullrich A, Bell JR, Chen EY, Herrera R, Petruzzelli LM, Dull TJ, Gray A, et al. Human insulin receptor and its relationship to the tyrosine kinase family of oncogenes. *Nature* 1985;313:756-761.
- Sun XJ, Rothenberg P, Kahn CR, Backer JM, Araki E, Wilden PA, Cahill DA, et al. Structure of the insulin receptor substrate IRS-1 defines a unique signal transduction protein. *Nature* 1991;352:73-77.
- Sun XJ, Crimmins DL, Myers MJ, Miralpeix M, White MF. Pleiotropic insulin signals are engaged by multisite phosphorylation of IRS-1. *Mol Cell Biol* 1993;13:7418-7428.
- Myers MG, Backer JM, Sun XJ, Shoelson S, Hu P, Schlessinger J, Yoakim M, et al. IRS-1 activates phosphatidylinositol 3'-kinase by associating with src homology 2 domains of p85. *Proc Natl Acad Sci U S A* 1992;89:10350-10354.
- Bonini JA, Colca JR, Dailey C, White M, Hofmann C. Compensatory alterations for insulin signal transduction and glucose transport in insulin-resistant diabetes. *Am J Physiol* 1995;269:E759-E765.

12. Kuhne MR, Zhao Z, Rowles J, Lavan BE, Shen SH, Fischer EH, Lienhard GE. Dephosphorylation of insulin receptor substrate 1 by the tyrosine phosphatase PTP2C. *J Biol Chem* 1994;269:15833-15837.
13. Backer JM, Myers MJ, Shoelson SE, Chin DJ, Sun XJ, Miralpeix M, Hu P, et al. Phosphatidylinositol 3'-kinase is activated by association with IRS-1 during insulin stimulation. *EMBO J* 1992;11:3469-3479.
14. Auer KL, Contessa J, Brenz-Verca S, Pirola L, Rusconi S, Cooper G, Abo A, et al. The Ras/Rac1/Cdc42/SEK/JNK/c-Jun cascade is a key pathway by which agonists stimulate DNA synthesis in primary cultures of rat hepatocytes. *Mol Biol Cell* 1986;9:561-573.
15. Baltensperger K, Kozma LM, Cherniack AD, Klarlund JK, Chawla A, Banerjee U, Czech MP. Binding of the Ras activator son of sevenless to insulin receptor substrate-1 signaling complexes. *Science* 1993;260:1950-1952.
16. Skolnik EY, Batzer A, Li N, Lee CH, Lowenstein E, Mohammadi M, Margolis B, et al. The function of GRB2 in linking the insulin receptor to Ras signaling pathways. *Science* 1993;260:1953-1955.
17. Burgering BM, Coffey PJ. Protein kinase B (c-Akt) in phosphatidylinositol-3-OH kinase signal transduction. *Nature* 1995;376:599-376602.
18. Coffey PJ, Jin J, Woodgett JR. Protein kinase B (c-Akt): a multifunctional mediator of phosphatidylinositol 3-kinase activation. *Biochem J* 1998;335:1-13.
19. Banerjee K, Mohr L, Wands JR, de la Monte SM. Ethanol inhibition of insulin signaling in hepatocellular carcinoma cells. *Alcohol Clin Exp Res* 1998;22:2093-2101.
20. Urso T, Gavalier JS, Van Thiel DH. Blood ethanol levels in sober alcohol users seen in an emergency room. *Life Sci* 1981;28:1053-1056.
21. Ausubel FM, Brent R, Kingston RE, Moore DD, Seidman JG, Smith JA, Struhl K. *Current Protocols in Molecular Biology*. New York: John Wiley & Sons, 2002.
22. Seglen PO. Preparation of isolated rat liver cells. *Methods Cell Biol* 1976;13:29-83.
23. Mao PL, Jiang Y, Wee BY, Porter AG. Activation of caspase-1 in the nucleus requires nuclear translocation of pro-caspase-1 mediated by its prodomain. *J Biol Chem* 1998;273:23621-23624.
24. Lingohr MK, Dickson LM, McCuaig JF, Hugl SR, Twardzik DR, Rhodes CJ. Activation of IRS-2-mediated signal transduction by IGF-1, but not TGF- α or EGF, augments pancreatic β -cell proliferation. *Diabetes* 2002;51:966-976.
25. Xiao H, Yin T, Wang XY, Uchida T, Chung J, White MF, Yang YC. Specificity of interleukin-2 receptor gamma chain superfamily cytokines is mediated by insulin receptor substrate-dependent pathway. *J Biol Chem* 2002;277:8091-8098.
26. Walker SM, Downes CP, Leslie NR. TPPI: a novel phosphoinositide 3-phosphatase. *Biochem J* 2001;360:277-283.
27. Torres J, Pulido R. The tumor suppressor PTEN is phosphorylated by the protein kinase CK2 at its C terminus. Implications for PTEN stability to proteasome-mediated degradation. *J Biol Chem* 2001;276:993-998.
28. Vazquez F, Ramaswamy S, Nakamura N, Sellers WR. Phosphorylation of the PTEN tail regulates protein stability and function. *Mol Cell Biol* 2000;20:5010-5018.
29. Singh B, Reddy PG, Goberdhan A, Walsh C, Dao S, Ngai I, Chou TC, et al. p53 Regulates cell survival by inhibiting PIK3CA in squamous cell carcinomas. *Genes Dev* 2003;16:984-993.
30. Brunet A, Bonni A, Zigmond MJ, Lin MZ, Juo P, Hu LS, Anderson MJ, et al. Akt promotes cell survival by phosphorylating and inhibiting a Forkhead transcription factor. *Cell* 1999;96:857-868.
31. Kawano T, Morioka M, Yano S, Hamada J, Ushio Y, Miyamoto E, Fukunaga K. Decreased akt activity is associated with activation of forkhead transcription factor after transient forebrain ischemia in gerbil hippocampus. *J Cereb Blood Flow Metab* 2002;22:926-934.
32. Muller M, Wilder S, Bannasch D, Israeli D, Lehlbach K, Li-Weber M, Friedman SL, et al. p53 Activates the CD95 (APO-1/Fas) gene in response to DNA damage by anticancer drugs. *J Exp Med* 1998;188:2033-2045.
33. Tamura T, Aoyama N, Saya H, Haga H, Futami S, Miyamoto M, Koh T, et al. Induction of Fas-mediated apoptosis in p53-transfected human colon carcinoma cells. *Oncogene* 1995;11:1939-1946.
34. Owen-Schaub LB, Zhang W, Cusack JC, Angelo LS, Santee SM, Fujiwara T, Roth JA, et al. Wild-type human p53 and a temperature-sensitive mutant induce Fas/APO-1 expression. *Mol Cell Biol* 1995;15:3032-3040.
35. Hong F, Nguyen VA, Shen X, Kunos G, Gao B. Rapid activation of protein kinase B/Akt has a key role in antiapoptotic signaling during liver regeneration. *Biochem Biophys Res Commun* 2002;279:974-979.
36. Kulik G, Klippel A, Weber MJ. Antiapoptotic signalling by the insulin-like growth factor I receptor, phosphatidylinositol 3-kinase, and Akt. *Mol Cell Biol* 1997;17:1595-1606.
37. Harwood AJ. Regulation of GSK-3: a cellular multiprocessor. *Cell* 2001;105:821-824.
38. Orena SJ, Torchia AJ, Garofalo RS. Inhibition of glycogen-synthase kinase 3 stimulates glycogen synthase and glucose transport by distinct mechanisms in 3T3-L1 adipocytes. *J Biol Chem* 2000;275:15765-15772.
39. Pap M, Cooper GM. Role of glycogen synthase kinase-3 in the phosphatidylinositol 3-Kinase/Akt cell survival pathway. *J Biol Chem* 1998;273:19929-19932.
40. Datta SR, Dudek H, Tao X, Masters S, Fu H, Gotoh Y, Greenberg ME. Akt phosphorylation of BAD couples survival signals to the cell-intrinsic death machinery. *Cell* 1997;91:231-241.
41. Condorelli F, Salomoni P, Cotteret S, Cesi V, Srinivasula SM, Alnemri ES, Calabretta B. Caspase cleavage enhances the apoptosis-inducing effects of BAD. *Mol Cell Biol* 2001;21:3025-3036.
42. Kennedy SG, Kandel ES, Cross TK, Hay N. Akt/Protein kinase B inhibits cell death by preventing the release of cytochrome c from mitochondria. *Mol Cell Biol* 1999;19:5800-5810.
43. Dajani R, Fraser E, Roe SM, Young N, Good V, Dale TC, Pearl LH. Crystal structure of glycogen synthase kinase 3 β : structural basis for phosphate-primed substrate specificity and autoinhibition. *Cell* 2001;105:721-732.
44. van Weeren PC, de Bruyn KM, de Vries-Smits AM, van Lint J, Burgering BM. Essential role for protein kinase B (PKB) in insulin-induced glycogen synthase kinase 3 inactivation. Characterization of dominant-negative mutant of PKB. *J Biol Chem* 1998;273:13150-13156.
45. Di Cristofano A, Pesce B, Cordon-Cardo C, Pandolfi PP. Pten is essential for embryonic development and tumour suppression. *Nat Genet* 1998;19:348-355.
46. Di Cristofano A, Pandolfi PP. The multiple roles of PTEN in tumor suppression. *Cell* 2000;100:387-390.
47. Dahia PL, Aguiar RC, Alberta J, Kum JB, Caron S, Sill H, Marsh DJ, et al. PTEN is inversely correlated with the cell survival factor Akt/PKB and is inactivated via multiple mechanisms in haematological malignancies. *Hum Mol Genet* 1999;8:185-193.
48. Lee JO, Yang H, Georgescu MM, Di Cristofano A, Maehama T, Shi Y, Dixon JE, et al. Crystal structure of the PTEN tumor suppressor: implications for its phosphoinositide phosphatase activity and membrane association. *Cell* 1999;99:323-334.
49. Maehama T, Dixon JE. PTEN: a tumour suppressor that functions as a phospholipid phosphatase. *Trends Cell Biol* 1999;9:125-128.
50. Wu X, Senechal K, Neshat MS, Whang YE, Sawyers CL. The PTEN/MMAC1 tumor suppressor phosphatase functions as a negative regulator of the phosphoinositide 3-kinase/Akt pathway. *Proc Natl Acad Sci U S A* 1998;95:15587-15591.
51. Huang J, Kontos CD. Inhibition of vascular smooth muscle cell proliferation, migration, and survival by the tumor suppressor protein PTEN. *Arterioscler Thromb Vasc Biol* 2002;22:745-751.
52. Kops GJ, Burgering BM. Forkhead transcription factors are targets of signalling by the proto-oncogene PKB (C-AKT). *J Anat* 2002;197:571-574.
53. Badoff C, Ruetten H, Mueller S, Stahmer M, Gehring D, Jung F, Ihling C, et al. Fas receptor signaling inhibits glycogen synthase kinase 3 beta and induces cardiac hypertrophy following pressure overload. *J Clin Invest* 2002;109:373-381.

54. Zhu Q, Meisinger J, Emanuele NV, Emanuele MA, LaPaglia N, Van Thiel DH. Ethanol exposure enhances apoptosis within the testes. *Alcohol Clin Exp Res* 2002;24:1550-1556.
55. Mansouri A, Gaou I, De Kerguenec C, Amsellem S, Haouzi D, Berson A, Moreau A, et al. An alcoholic binge causes massive degradation of hepatic mitochondrial DNA in mice. *Gastroenterology* 1999;117:181-190.
56. de la Monte SM, Ganju N, Banerjee K, Brown NV, Luong T, Wands JR. Partial rescue of ethanol-induced neuronal apoptosis by growth factor activation of phosphoinositol-3-kinase. *Alcohol Clin Exp Res* 2000;24:716-726.
57. Lumpkin CK Jr, Moore TL, Tarpley MD, Taylor JM, Badger TM, McClung JK. Acute ethanol and selected growth suppressor transcripts in regenerating rat liver. *Alcohol* 1995;12:357-362.
58. Kim JM, Yoon YD, Tsang BK. Involvement of the Fas/Fas ligand system in p53-mediated granulosa cell apoptosis during follicular development and atresia. *Endocrinology* 1999;140:2307-2317.